analytical chemistry

Article

pubs.acs.org/ac

Hybridization Chain Reaction Amplification of MicroRNA Detection with a Tetrahedral DNA Nanostructure-Based Electrochemical Biosensor

Zhilei Ge,[†,∥] Meihua Lin,[†,∥] Ping Wang,[‡] Hao Pei,[†] Juan Yan,[‡] Jiye Shi,[§] Qing Huang,[†] Dannong He,[‡] Chunhai Fan,[†] and Xiaolei Zuo*[,†]

[†]Division of Physical Biology & Bioimaging Center, Shanghai Synchrotron Radiation Facility, Shanghai Institute of Applied Physics, Chinese Academy of Sciences, Shanghai 201800, China

[‡]National Engineering Research Center for Nanotechnology, Shanghai 200241, China

[§]UCB Pharma, Slough SL1 3WE, United Kingdom

Supporting Information

ABSTRACT: There remains a great challenge in the sensitive detection of microRNA because of the short length and low abundance of microRNAs in cells. Here, we have demonstrated an ultrasensitive detection platform for microRNA by combining the tetrahedral DNA nanostructure probes and hybridization chain reaction (HCR) amplification. The detection limits for DNA and microRNA are 100 aM and 10 aM (corresponding to 600 microRNAs in a 100 μL sample), respectively. Compared to the widely used supersandwich amplification, the detection limits are improved by 3 orders of magnitude. The uncontrolled surface immobilization and consumption of target molecules that limit the amplification efficiency of supersandwich are eliminated in our platform. Taking advantage of DNA nanotechnology, we employed three-dimensional tetrahedral DNA nanostructure as the scaffold to immobilize DNA recognition probes to increase the reactivity and accessibility, while DNA nanowire tentacles are used for efficient signal amplification by capturing multiple catalytic enzymes in a highly ordered way. The synergetic effect of DNA tetrahedron and nanowire tentacles have proven to greatly improve sensitivity for both DNA and microRNA detection.

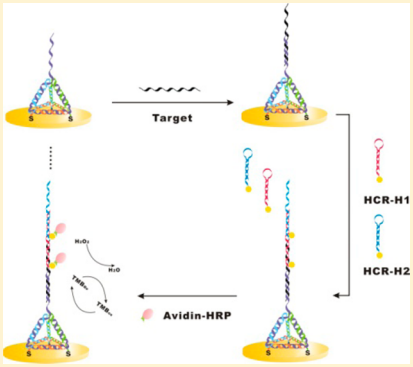

MicroRNAs, a class of small noncoding RNAs, play critical regulatory functions in many biological processes such as cell differentiation and cell apoptosis.[1−4] Recently, accumulated evidence has proven that microRNAs are highly correlated to cancers, which indicates microRNAs are informative enough to distinguish between tumor and normal tissues. More recently, the presence of microRNAs in serum has been clearly demonstrated too.[5,6] Therefore, microRNAs have become clinically important biomarkers for early cancer diagnostic and prognostic processes.[1,2,7−9]

However, there remain major challenges in the sensitive and selective detection of microRNAs.[9−12] One of the main challenges is the small size (usually 18−24 nucleotides) of these tiny microRNAs. The short length of microRNAs requires the design of short primers for the classic and sensitive PCR (polymerase chain reaction) methods to analyze microRNAs. This in turn decreases the efficiency of PCR and increases the chances of nonspecific amplification. The other challenge is the low abundance of microRNAs in cells and circulating blood. Hence, the Northern blotting method, the gold standard method for microRNA analysis, has a problem of low detection sensitivity (usually in nanomoles). Although microarray has the advantage of high throughput, microarray technologies are also limited by the problems of undesired cross-hybridization and low sensitivity. Hence, a simple and sensitive detection platform is urgently needed for the microRNA analysis.[10]

Electrochemical biosensors are well recognized as promising candidates for rapid, inexpensive, miniaturized detection devices (for example, the well-commercialized electrochemical glucose meter for personal use).[7,13−33] However, a challenge in electrochemical biosensor design is the control of density and orientation of recognition probes at the surface.[16,17,20,22,27,32,34−36] Usually, overall performance of the biosensor is negatively affected by the crowding effect or steric effect, entanglement of probes, nonspecific interactions between probes, and surface defects in the self-assembled monolayer. To improve the situation, some diluent small molecules are involved in the assembly process.[32] On the other hand, some nanostructured surfaces are designed to overcome the influence of dense probe packing and enhance mass transport.[20,22,27] However, these technologies suffer from multiple steps and complicated nanofabrication. To address this problem, our group has used DNA tetrahedra as a scaffold

Received: November 16, 2013
Accepted: January 22, 2014
Published: January 22, 2014

   dx.doi.org/10.1021/ac4037262 | *Anal. Chem.* 2014, 86, 2124−2130

to construct "bottom-up" anchor bioprobes with well-controlled nanoscale distance between probes and orientation.[7,14,16,17,28] Thus, the sensing ability is improved significantly.

The same challenge also limits the efficiency of signal amplification and the sensitivity. A large number of signaling molecules such as enzymes are commonly immobilized on various nanomaterials to amplify the signal. Uncontrolled and unordered surface immobilization would decrease the efficiency of enzyme reactions. Recently, supersandwich structure has been widely used as an efficient signal amplification that represents a significant improvement in biosensor design. However, uncontrolled surface modification and the consumption of target molecules in the formation of supersandwich structure limit its efficiency of amplification.[18,37−39] Hybridization chain reaction (HCR) is a novel amplification method via triggered cascade of DNA polymerization by initiator or target molecules.[8,40−48] Importantly, the products of HCR are DNA double helices that are highly ordered. The signaling molecules can be attached on these helices with precisely controlled density, which should be beneficial for the final amplification efficiency.

Here, we further investigate the combination of DNA tetrahedral platform and HCR amplification (Figure 1).

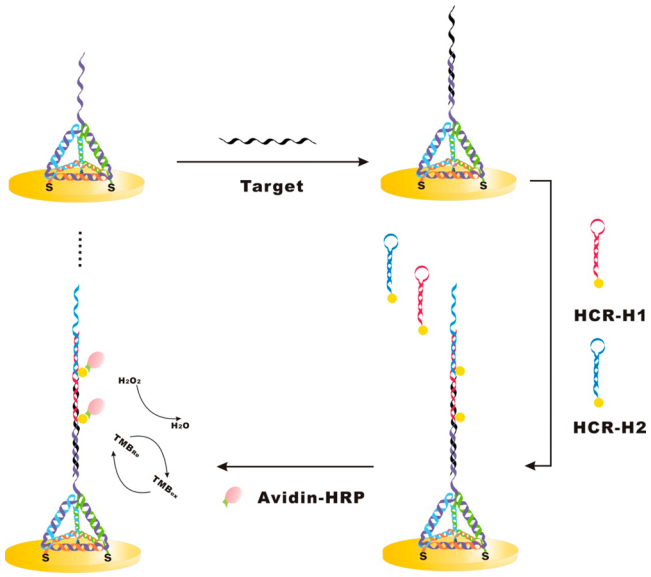

Figure 1. Schematic illustration of electrochemical DNA detection. Probes are immobilized on a 3D tetrahedral scaffold, and signal is amplified by hybridization chain reaction (HCR). The synergetic effect of tetrahedral probes and HCR improves the detection sensitivity greatly. First, the target was used to hybridize with the tetrahedral probes on the surface. Then, biotin-modified H1 and H2 were used to amplify the hybridization signal by adding amplified chain on each target. Finally, the avidin-modified HRP was attached on the HCR products that can produce an electrocatalytic signal.

Through the synergetic effect of tetrahedron scaffold and HCR, the detection sensitivity is greatly improved to 100 aM for DNA detection and 10 aM for microRNA detection (corresponding to 600 microRNAs in a 100 μL sample).

EXPERIMENTAL SECTION

Chemical and Reagents. All oligonucleotides were synthesized and purified by Invitrogen Inc. (Shanghai, China), and the sequences are shown in Table 1. Ethylenediaminetetraacetic acid (EDTA), tris(2-carboxyethyl)-phosphine hydrochloride (TCEP), and diethyl pyrocarbonate (DEPC) were purchased from Sigma−Aldrich (St. Louis, MO). TMB substrate (3,3′,5,5′-tetramethylbenzidine; Neogen K-blue low-activity substrate) was purchased from Neogen. Avidin−HRP (horseradish peroxidase) was purchased from Roche Diagnostics (Mannheim, Germany). All solutions were prepared with Milli-Q water (18 MΩ·cm resistivity) from a Millipore system.

Self-Assembly of DNA Tetrahedron-Structured Probes at Gold Electrode Surfaces. Gold electrodes were cleaned following the reported protocol.[49] Four strands, tetrahedron A, B, C, and D, were dissolved in TM buffer (10 mM Tris-HCl and 50 mM $MgCl_2$, pH 8.0), yielding a final concentration of 50 μM. Two microliters of each strand was combined with 10 μL of TCEP (30 mM) and 82 μL TM buffer, and the resulting mixture was heated to 95 °C for 2 min and then cooled to 4 °C over 30 s by use of a Peltier thermal cycler PTC-200 (MJ Research Inc., SA). The final concentration of tetrahedron-structured probes (TSP) is 1 μM. After that, 3 μL of TSP was added to the cleaned gold electrode and allowed to react overnight at room temperature. The electrode was rinsed with 0.01 M phosphate-buffered saline (PBS). The surface density was calculated by our established method[14] and we obtained 3.2×10^{12} tetrahedra·cm^{-2}. The distance between probes is ∼5.6 nm.

Native Gel Electrophoresis. H1 and H2 samples were heated to 95 °C for 2 min and then allowed to cool to room temperature for 1 h before use. The 1% agarose gels contained 0.5 μg of ethidium bromide/mL of gel volume and were prepared with 1× TAE buffer (40 mM Tris−acetate and 1 mM EDTA, pH 8.0) and were run at 150 V for 60 min and visualized under UV light.

Quartz Crystal Microbalance Measurements. All quartz crystal microbalance (QCM) experiments were performed at 25 °C with a quartz crystal microbalance (D300, Q-Sense, Gothenburg, Sweden) to measure DNA binding at TSP-modified gold surfaces.

TSP DNA structures (1 μM) in TM buffer were prepared and then automatically deposited on Au film to get a well-aligned biolayer. Then the target solution was injected into the chamber. After that, we injected the solution of H1 or H2 alternatively for each step, so we could monitor each addition step in real time. The volume of each injection is 1 mL, so the unbound reactant from the last step will be totally rinsed off because the capacity of the reaction chamber is only ∼200 μL.

DNA and MicroRNA Detection. DNA detection was carried out in the sandwich format. The target DNA was first hybridized with the capture probe (fragments of tetrahedron A) on Au surface in 1× SPSC buffer (1 M NaCl and 50 mM Na_2HPO_4, pH 7.5). At the meantime, 1 μM H1 and 1 μM H2 were heated separately to 95 °C for 5 min, allowed to cool on ice for 15 min, and then mixed together in 1× SPSC buffer for the final concentration 100 nM before use. After 2 h incubation with the target DNA at room temperature, the electrodes were rinsed by 0.01 M PBS buffer and then incubated with the mixture of H1 and H2 for the HCR. After another 2 h of reaction, the electrodes was dipped with 3 μL of avidin−HRP (0.5 unit/mL) for 15 min at room temperature and then rinsed to be ready for the electrochemical measurements.

The same strategy was used for microRNA detection: first, heated microRNA-helper was heated to 95 °C for 5 min and

dx.doi.org/10.1021/ac4037262 | Anal. Chem. 2014, 86, 2124−2130

Table 1. DNA and MicroRNA Sequences Employed in This Work

oligonucleotide	sequence (5′−3′)
tetrahedron A	ACATTCCTAAGTCTGAAACATTACAGCTTGCTACACGAGAAGAGCCGCCATAGTATTTTTTTTTTGTATCCAGTGGCTCAGACTTTTGAC
tetrahedron B	SH-TATCACCAGGCAGTTGACAGTGTAGCAAGCTGTAATAGATGCGAGGGTCCAATAC
tetrahedron C	SH-TCAACTGCCTGGTGATAAAACGACACTACGTGGGAATCTACTATGGCGGCTCTTC
retrahedron D	SH-TTCAGACTTAGGAATGTGCTTCCCACGTAGTGTCGTTTGTATTGGACCCTCGCAT
DNA target	AGTCTAGGATTCGGCGTGGGTTAAGTCAAAAGTCTGAGCCACTGGATAC
H1	biotin-TTAACCCACGCCGAATCCTAGACTCAAAGTAGTCTAGGATTCGGCGTG
H2	AGTCTAGGATTCGGCGTGGGTTAACACGCCGAATCCTAGACTACTTTG-biotin
microRNA-122b	UGGAGUGUGACAAUGGUGUUUGA
microRNA-helper	GTCAAAAGTCTGAGCCACTGGATACTCAAACACCATTGTCACACTCCAGCAATTTGGAGTGTGACAATGGT
microRNA-H1	TGGAGTGTGACAATGGTGTTTGAACCATTGTCACACTCCACGTTAA-biotin
microRNA-H2	biotin-TCAAACACCATTGTCACACTCCAGCAATTTGGAGTGTGACAATGGT
capture probe of supersandwich	CGGC ACC TGG GGG AGT ATT GCG GAG GAA GGT GCCG
target of supersandwich	T ACTCCCCCAGGT GCCG A CGGC ACCTTCCTCCGC A

allowed to cool on ice for 15 min, and then the electrodes were incubated in microRNA 122b solution to initiate the HCR amplification. This time we used DEPC-treated Milli-Q water instead of Milli-Q water as the solvent, and also every step, including assembly and polymerization processes, was performed at a clean bench.

Electrochemical Measurements. Electrochemical measurements were performed with a Model CHI 630 electrochemical workstation (CH Instruments, Inc., Austin, TX) and a conventional three-electrode configuration was employed throughout the experiment, which involved a gold working electrode, a platinum wire auxiliary electrode, and an Ag/AgCl (3 M KCl) reference electrode. Cyclic voltammetry (CV) was carried out at a scan rate of 50 mV/s. Amperometric detection was fixed at 150 mV, and the electroreduction current was measured 100 s after the HRP redox reaction reached steady state.

RESULTS AND DISCUSSION

The HCR reactions are realized through triggered hairpin polymerization, where we use our target DNA as an initiator and two biotin-labeled hairpins (H1 and H2) as fuel strands. Through our rational design, the hairpin structure has a short loop region and a long stem region that ensure a thermodynamic steady state (Table S1, Supporting Information). In the absence of the initiator (target DNA), the two hairpins fold into hairpin structures separately in solution (Figure 2A). By introducing the initiator, the steady state is disturbed by the hybridization of initiator and H1, and thus the HCR reaction is triggered by alternating addition of these two hairpins (Figure 2A). Finally, the polymerization stops when the supply of these two hairpins is exhausted. We first investigate the polymerization reaction in solution and find out that the average length of products is inversely related to the concentration of initiator. When we use higher concentration of initiator, more H1 are opened spontaneously and then more parallel polymerization reactions occur spontaneously, resulting in shorter products. When we decrease the concentration of initiator, the length of products becomes longer (Figure 2A). Importantly, the longest product is over 2000 base pairs, which should be highly efficient for signal amplification. As a sharp contrast, the length of supersandwich structures is less than 1000 base pairs (most supersandwich structures are less than 500 base pairs in length) (Figure 2B). The average length of supersandwich structures decreases along

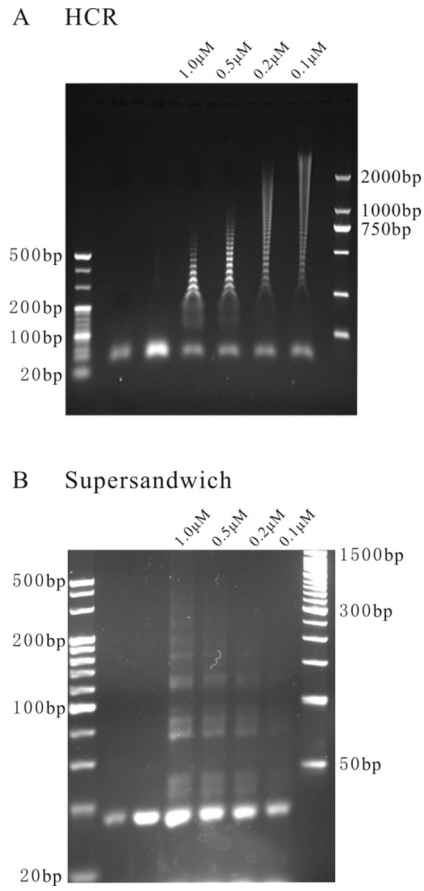

Figure 2. (A) Effect of initiator concentrations on HCR. Lanes 1 and 8, 20-bp and 2000-bp DNA ladder markers, respectively; lane 2, 1.0 μM H1; lanes 3−7, five different concentrations of initiator (0.0, 1.0, 0.50, 0.20, and 0.10 μM) in a 1 μM mixture of H1 and H2. (B) Effect of target concentrations on supersandwich structure. Lanes 1 and 8, 20-bp and 50-bp DNA ladder markers, respectively; lane 2, capture probe; lane 3, target probe; lanes 4−7, four different concentrations of target probe (1.0, 0.50, 0.20, and 0.10 μM) in solution of 10 μM capture probe.

with decreasing target concentration that limits the amplification efficiency at low concentration of target (Figure 2B).

Then, to fully understand the mechanism of HCR amplification at the bionanointerface, we transferred the HCR amplification from solution to tetrahedral probe-modified gold

dx.doi.org/10.1021/ac4037262 | Anal. Chem. 2014, 86, 2124−2130

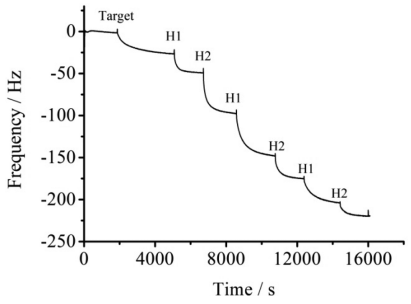

Figure 3. Change of resonant frequency as a function of time on tetrahedral probe-modified gold surface. After the target strand hybridized with probes on surface, H1 (1 μM) or H2 (1 μM) was added in the reaction cell alternatively, and each step was achieved until the frequency was steady. For each step, the volume of injection was 1 mL. The temperature was controlled at 25 °C with a quartz crystal microbalance.

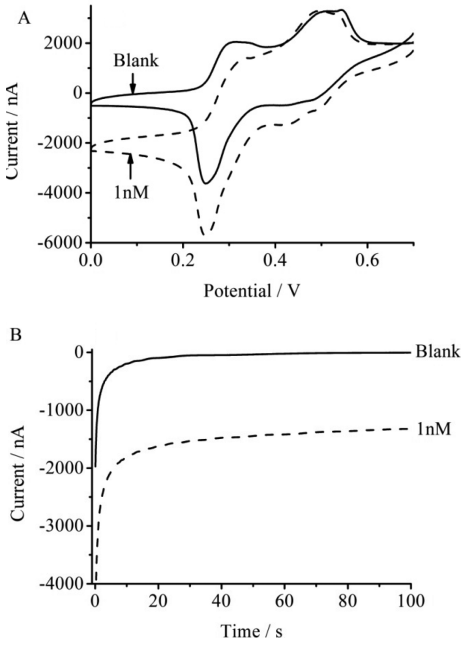

Figure 4. (A) Cyclic voltammograms (CVs) for tetrahedral probe-based electrochemical sensor in the absence (—) and presence (---) of 1 nM target DNA. Scan rate: 50 mV/s. The representative redox peaks of TMB were observed and the increasing electrocatalytic current indicated successful target detection. (B) Amperometric response of 0 (—) and 1 nM (---) target DNA on tetrahedral probe-based sensor. The potential was held at 150 mV (vs Ag/AgCl) and the reduction current was recorded at 100 s.

surface. We use quartz crystal microbalance (QCM), which is sensitive enough to monitor the real-time polymerization. Interestingly, we observe a real-time process of target hybridization and the alternating addition of hairpins on the tetrahedral probes. For each addition step, it takes only ~20 min to get a near-saturated signal that is rapid (Figure 3). The efficiency of the first addition step is over 90% according to the calculation of mass change on the gold surface. This high efficiency originates from the highly ordered tetrahedral probes. On the uncontrolled linear probe-modified gold surface, the hybridization efficiency is much lower than 90%.[22,27] We collect the data from six additional steps here to show the successful HCR amplification on the tetrahedral bionanointerface. The

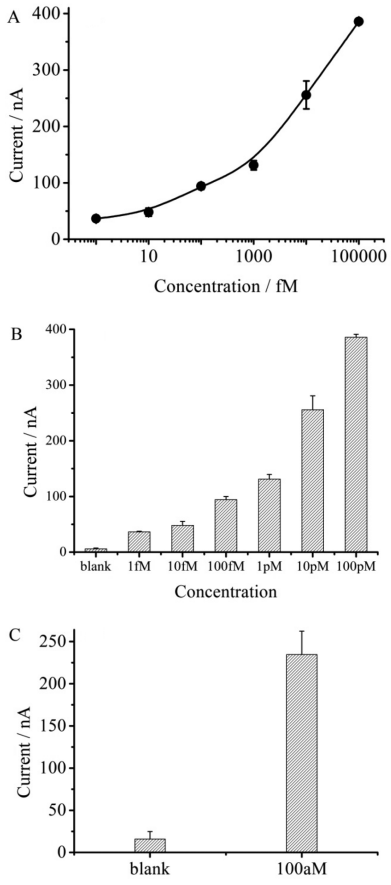

Figure 5. (A) Logarithmic plot of amperometric current versus DNA concentration for tetrahedral probe-based electrochemical sensor. (B) Concentration profile for detection. The current increases along with increasing target concentration. Error bars represent standard deviations for measurements taken from at least three independent experiments. (C) By increasing the hybridization time of target DNA and probes from 2 to 4 h and also increasingthe polymerization time from 2 to 12 h, a significant signal difference between 0 and 100 aM target can be obtained.

incorporation of biotin labels in the fuel strands will be used to capture avidin-modified horseradish peroxidase (HRP).

With the successful HCR on the bionanointerface, we design a DNA detection system that combines tetrahedral probes and HCR amplification (Figure 1). In our system, the tetrahedral probes ensure immobilization with well-controlled density and orientation. The nicked double helices from HCR are used to capture multiple HRP enzymes that amplify the final electrochemical signal through the catalytic reaction of H_2O_2. The synergetic combination of tetrahedral probes and HCR would improve the detection sensitivity of nucleic acids.

Then we try to detect target DNA by using this system. In the presence of target DNA (1 nM), we observe an apparent increase in current from cyclic voltammetry, leading to a pair of asymmetric redox peaks that are characteristic of the occurrence of an electrocatalytic reaction (Figure 4A). As a contrast, without target DNA, two pairs of well-defined redox peaks that are assigned to the typical two-electron redox reaction of TMB (3,3′,5,5′-tetramethylbenzidine, an electron-transfer mediator in enzyme catalytic reaction). To quantify the electrochemical signal, we use the $I-t$ curve to measure the current from the elecrocatalytic reaction. We obtain a current of 1300 nA when we detect the target DNA of 1 nM, which is 250

dx.doi.org/10.1021/ac4037262 | Anal. Chem. 2014, 86, 2124−2130

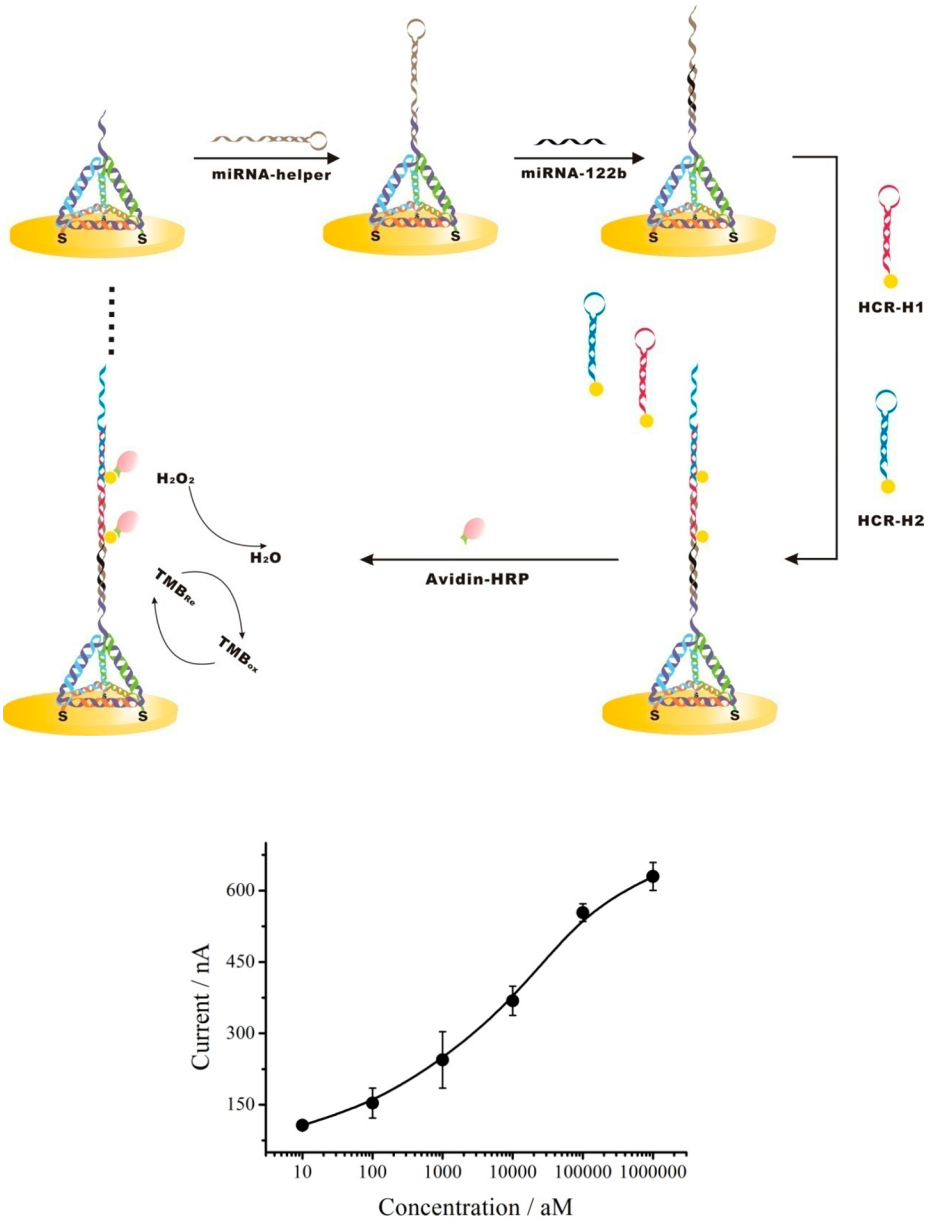

Figure 6. (top) The detection principle is similar to what we used in DNA detection, whereas we introduce a DNA helper that can not only act as a bridge but also fold into a stem–loop structure itself to avoid nonspecific reaction. By taking advantage of the amplification via HCR amplification, we achieved ultrasensitive microRNA detection. (bottom) Increasing electrochemical current versus target concentration. The dynamic range is broad and spans from 10 aM to 1 pM.

times higher than the current (~5 nA) without the target DNA (Figure 4B). This relatively large difference makes our detection sensitive. We can detect the target DNA as low as 1 fM, and above this concentration the electrochemical current increases monotonically along with the increase of concentration of target DNA. The dynamic range of our detection spans 5 orders of magnitude, from 1 fM to 100 pM (Figure 5A,B). We further challenged our system with a target DNA of 100 aM, and we found that such a low concentration can be detected sensitively with a longer amplification time (~12 h, Figure 5C). One unique characteristic of HCR reaction is that the length of reaction product keep increasing when the target concentration keeps decreasing, which means the HCR amplification is ultrasensitive when the target concentration is low. So a large number of HRPs were attached on the long amplified chain to produce detectable electrocatalytic signal when the target concentration is as low as 100 aM.

We further generalize our detection platform to the detection of microRNA because of the significant importance of microRNA in cancer development and diagnostics. Because microRNAs are usually short, we creatively introduce a DNA hairpin structure named helper strand that is immobilized on the tetrahedron. In the presence of microRNA, the helper hairpin structure is open at first and then the HCR is initiated (Figure 6). With this design, impressively, microRNA as low as 10 aM can be sensitively detected (Figure 6; Figures S1 and S2, Supporting Information).

Taking advantage of the tetrahedral structure, we employed three-dimensional tetrahedral DNA nanostructure as the scaffold to immobilize DNA recognition probes to increase the reactivity and accessibility. The use of tetrahedral probes

dx.doi.org/10.1021/ac4037262 | Anal. Chem. 2014, 86, 2124–2130

reduces the immobilization steps without the requirement of a "backfilling" process [for example, the use of 6-mercapto-1-hexanol (MCH) as backfiller].[32,49,50] Compared to some amplified detections for nucleic acids based on traditional linear probes such as supersandwich assay,[18,37,38] the detection limit is greatly improved from 100 fM to 100 aM for DNA detection and to 10 aM for microRNA detection. On the other hand, when compared to detection with tetrahedral probes, the HCR amplifies the final signal efficiently because the catalytic enzymes are introduced in a highly ordered way.[16] The detection limit is improved by several orders of magnitude. So this impressive improvement benefits from the synergetic effect of tetrahedral probes and HCR amplification. Our detection sensitivity is comparable to that of detection based on the finely controlled nanostructured surface.[20,22,27] However, our design is based only on DNA polymerization, which is cheap, programmable, and easy to operate, avoiding complicated micro/nanofabrications. Our tetrahedron is synthesized in one step, in one pot, and in several minutes with high uniformity and productivity that ensures our detection has high reproducibility.

■ ASSOCIATED CONTENT

Ⓢ Supporting Information

One table showing hairpin stability and two figures showing microRNA detection as low as 10 aM and a theoretical model to calculate accumulation time of target molecules on the nanostructured surface. This material is available free of charge via the Internet at http://pubs.acs.org.

■ AUTHOR INFORMATION

Corresponding Author

*E-mail zuoxiaolei@sinap.ac.cn.

Author Contributions

‖Z.G. and M.L. contributed equally.

Notes

The authors declare no competing financial interest.

■ ACKNOWLEDGMENTS

This work was supported by 100 talent project from Chinese Academy of Sciences, Shanghai Pujiang Project (No. 13PJ1410700), and the National Basic Research Program of China (973 program, No. 2012CB932600).

■ REFERENCES

(1) Lu, J.; Getz, G.; Miska, E. A.; Alvarez-Saavedra, E.; Lamb, J.; Peck, D.; Sweet-Cordero, A.; Ebet, B. L.; Mak, R. H.; Ferrando, A. A.; Downing, J. R.; Jacks, T.; Horvitz, H. R.; Golub, T. R. *Nature* **2005**, *435*, 834.

(2) Pritchard, C. C.; Cheng, H. H.; Tewari, M. *Nat. Rev. Genet.* **2012**, *13*, 358.

(3) Bartel, D. P. *Cell* **2004**, *116*, 281.

(4) Lewis, B. P.; Shih, I. H.; Jones-Rhoades, M. W.; Bartel, D. P.; Burge, C. B. *Cell* **2003**, *115*, 787.

(5) Mitchell, P. S.; Parkin, R. K.; Kroh, E. M.; Fritz, B. R.; Wyman, S. K.; Pogosova-Agadjanyan, E. L.; Peterson, A.; Noteboom, J.; O'Briant, K. C.; Allen, A.; Lin, D. W.; Urban, N.; Drescher, C. W.; Knudsen, B. S.; Stirewalt, D. L.; Gentleman, R.; Vessella, R. L.; Nelson, P. S.; Martin, D. B.; Tewari, M. *Proc. Natl. Acad. Sci. U.S.A.* **2008**, *105*, 10513.

(6) Song, M. Y.; Pan, K. F.; Su, H. J.; Zhang, L.; Ma, J. L.; Li, J. Y.; Yuasa, Y.; Kang, D.; Kim, Y. S.; You, W. C. *PLoS One* **2012**, *7*, No. e33608.

(7) Wen, Y. L.; Pei, H.; Shen, Y.; Xi, J. J.; Lin, M. H.; Lu, N.; Shen, X. Z.; Li, J.; Fan, C. H. *Sci. Rep.* **2012**, *2*, No. 867.

(8) Yang, L.; Liu, C.; Ren, W.; Li, Z. *ACS Appl. Mater. Interfaces* **2012**, *4*, 6450.

(9) Duan, R. X.; Zuo, X. L.; Wang, S. T.; Quan, X. Y.; Chen, D. L.; Chen, Z. F.; Jiang, L.; Fan, C. H.; Xia, F. *J. Am. Chem. Soc.* **2013**, *135*, 4604.

(10) Koshiol, J.; Wang, E.; Zhao, Y. D.; Marincola, F.; Landi, M. T. *Cancer Epidemiol., Biomarkers Prev.* **2010**, *19*, 907.

(11) Leshkowitz, D.; Horn-Saban, S.; Parmet, Y.; Feldmesser, E. *RNA* **2013**, *19*, 527.

(12) Harcourt, E. M.; Kool, E. T. *Nucleic Acids Res.* **2012**, *40*, e65.

(13) Pelossof, G.; Tel-Vered, R.; Elbaz, J.; Willner, I. *Anal. Chem.* **2010**, *82*, 4396.

(14) Lu, N.; Pei, H.; Ge, Z. L.; Simmons, C. R.; Yan, H.; Fan, C. H. *J. Am. Chem. Soc.* **2012**, *134*, 13148.

(15) Slinker, J. D.; Muren, N. B.; Renfrew, S. E.; Barton, J. K. *Nat. Chem.* **2011**, *3*, 228.

(16) Pei, H.; Lu, N.; Wen, Y. L.; Song, S. P.; Liu, Y.; Yan, H.; Fan, C. H. *Adv. Mater.* **2010**, *22*, 4754.

(17) Wen, Y. L.; Pei, H.; Wan, Y.; Su, Y.; Huang, Q.; Song, S. P.; Fan, C. H. *Anal. Chem.* **2011**, *83*, 7418.

(18) Xia, F.; White, R. J.; Zuo, X. L.; Patterson, A.; Xiao, Y.; Kang, D.; Gong, X.; Plaxco, K. W.; Heeger, A. J. *J. Am. Chem. Soc.* **2010**, *132*, 14346.

(19) Liu, G.; Wan, Y.; Gau, V.; Zhang, J.; Wang, L.; Song, S.; Fan, C. *J. Am. Chem. Soc.* **2008**, *130*, 6820.

(20) Soleymani, L.; Fang, Z. C.; Lam, B.; Bin, X. M.; Vasilyeva, E.; Ross, A. J.; Sargent, E. H.; Kelley, S. O. *ACS Nano* **2011**, *5*, 3360.

(21) Slinker, J. D.; Muren, N. B.; Gorodetsky, A. A.; Barton, J. K. *J. Am. Chem. Soc.* **2010**, *132*, 2769.

(22) Bin, X. M.; Sargent, E. H.; Kelley, S. O. *Anal. Chem.* **2010**, *82*, 5928.

(23) Farjami, E.; Clima, L.; Gothelf, K.; Ferapontova, E. E. *Anal. Chem.* **2011**, *83*, 1594.

(24) Xia, F.; Zuo, X. L.; Yang, R. Q.; Xiao, Y.; Kang, D.; Vallee-Belisle, A.; Gong, X.; Heeger, A. J.; Plaxco, K. W. *J. Am. Chem. Soc.* **2010**, *132*, 1252.

(25) Ferapontova, E. E.; Gothelf, K. V. *Electroanalysis* **2009**, *21*, 1261.

(26) Xiang, Y.; Lu, Y. *Anal. Chem.* **2012**, *84*, 4174.

(27) Soleymani, L.; Fang, Z. C.; Sargent, E. H.; Kelley, S. O. *Nat. Nanotechnol.* **2009**, *4*, 844.

(28) Pei, H.; Wan, Y.; Li, J.; Hu, H. Y.; Su, Y.; Huang, Q.; Fan, C. H. *Chem. Commun.* **2011**, *47*, 6254.

(29) Ferapontova, E. E.; Olsen, E. M.; Gothelf, K. V. *J. Am. Chem. Soc.* **2008**, *130*, 4256.

(30) Farjami, E.; Campos, R.; Nielsen, J. S.; Gothelf, K. V.; Kjems, J.; Ferapontova, E. E. *Anal. Chem.* **2013**, *85*, 121.

(31) Liu, X. Q.; Niazov-Elkan, A.; Wang, F. A.; Willner, I. *Nano Lett.* **2013**, *13*, 219.

(32) Wu, J.; Campuzano, S.; Halford, C.; Haake, D. A.; Wang, J. *Anal. Chem.* **2010**, *82*, 8830.

(33) Xiang, Y.; Lu, Y. *Nat. Chem.* **2011**, *3*, 697.

(34) Opdahl, A.; Petrovykh, D. Y.; Kimura-Suda, H.; Tarlov, M. J.; Whitman, L. J. *Proc. Natl. Acad. Sci. U.S.A.* **2007**, *104*, 9.

(35) Fu, J. L.; Liu, M. H.; Liu, Y.; Yan, H. *Acc. Chem. Res.* **2012**, *45*, 1215.

(36) Pinheiro, A. V.; Nangreave, J.; Jiang, S. X.; Yan, H.; Liu, Y. *ACS Nano* **2012**, *6*, 5521.

(37) Jiang, Y. N.; Liu, N. N.; Guo, W.; Xia, F.; Jiang, L. *J. Am. Chem. Soc.* **2012**, *134*, 15395.

(38) Liu, N. N.; Jiang, Y. N.; Zhou, Y. H.; Xia, F.; Guo, W.; Jiang, L. *Angew. Chem., Int. Ed.* **2013**, *52*, 2007.

(39) Takeuchi, T.; Matile, S. *J. Am. Chem. Soc.* **2009**, *131*, 18048.

(40) Zhu, G. Z.; Zhang, S. F.; Song, E. Q.; Zheng, J.; Hu, R.; Fang, X. H.; Tan, W. H. *Angew. Chem., Int. Ed.* **2013**, *52*, 5490.

(41) Huang, F. J.; You, M. X.; Han, D.; Xiong, X. L.; Liang, H. J.; Tan, W. H. *J. Am. Chem. Soc.* **2013**, *135*, 7967.

(42) Zhang, B.; Liu, B. Q.; Tang, D. P.; Niessner, R.; Chen, G. N.; Knopp, D. *Anal. Chem.* **2012**, *84*, 5392.
(43) Choi, J.; Love, K. R.; Gong, Y.; Gierahn, T. M.; Love, J. C. *Anal. Chem.* **2011**, *83*, 6890.
(44) Chen, Y.; Xu, J.; Su, J.; Xiang, Y.; Yuan, R.; Chai, Y. *Anal. Chem.* **2012**, *84*, 7750.
(45) Choi, H. M. T.; Chang, J. Y.; Trinh, L. A.; Padilla, J. E.; Fraser, S. E.; Pierce, N. A. *Nat. Biotechnol.* **2010**, *28*, 1208.
(46) Huang, J.; Wu, Y. R.; Chen, Y.; Zhu, Z.; Yang, X. H.; Yang, C. J.; Wang, K. M.; Tan, W. H. *Angew. Chem., Int. Ed.* **2011**, *50*, 401.
(47) Zheng, J.; Zhu, G. Z.; Li, Y. H.; Li, C. M.; You, M. X.; Chen, T.; Song, E. Q.; Yang, R. H.; Tan, W. H. *ACS Nano* **2013**, *7*, 6545.
(48) Dirks, R. M.; Pierce, N. A. *Proc. Natl. Acad. Sci. U.S.A.* **2004**, *101*, 15275.
(49) Lao, R. J.; Song, S. P.; Wu, H. P.; Wang, L. H.; Zhang, Z. Z.; He, L.; Fan, C. H. *Anal. Chem.* **2005**, *77*, 6475.
(50) Zhang, J.; Lao, R. J.; Song, S. P.; Yan, Z. Y.; Fan, C. H. *Anal. Chem.* **2008**, *80*, 9029.